

The semileptonic $\bar{B} \rightarrow D\ell\bar{\nu}$ and $\bar{B}_s \rightarrow D_s\ell\bar{\nu}$ decays in Isgur–Wise approach

H. Hassanabadi^{1,a}, S. Rahmani¹, S. Zarrinkamar²

¹ Physics Department, Shahrood University, Shahrood, Iran

² Department of Basic Sciences, Garmsar Branch, Islamic Azad University, Garmsar, Iran

Received: 16 July 2014 / Accepted: 26 September 2014 / Published online: 10 October 2014

© The Author(s) 2014. This article is published with open access at Springerlink.com

Abstract We consider a combination of linear confining and Hulthén potentials in the Hamiltonian and, via the perturbation approach, report the corresponding Isgur–Wise function parameters. Next, we investigate the Isgur–Wise function for $\bar{B} \rightarrow D\ell\bar{\nu}$ and $\bar{B}_s \rightarrow D_s\ell\bar{\nu}$ semileptonic decays and report the decay width, branching ratio, and $|V_{cb}|$ CKM matrix element. A comparison with other models and experimental values is included.

1 Introduction

The semileptonic B to D mesonic decay is the focus of many current studies in the annals of particle physics. Although a plethora of approaches have been applied to the field, the relatively old but powerful Isgur–Wise function (IWF) approach is a good candidate for use to analyze the problem. Isgur and Wise obtained simple and appealing relations of the form factors for weak pseudoscalar to pseudoscalar and pseudoscalar to vector transitions for various hadronic matrix elements [1, 2]. If $m_Q \gg \Lambda_{\text{QCD}}$ (m_Q is the heavy-quark mass and Λ_{QCD} is QCD scale parameter), the number of form factors in semileptonic decay reduces. Next, all form factors of semileptonic decays in the heavy-quark limit can be defined in terms of a single universal function, i.e. the IWF [3]. The main part of the IWF includes the wave function of the meson and some kinematic factors, which depend on the four velocities of heavy-light mesons before and after recoil. The calculation of the IWF is the essential step in all calculations of the branching ratios, V_{cb} element of the CKM matrix, decay rates, and branching ratios [4]. To get the V_{cb} element of the CKM matrix we can use the IWF by the experimental data on V_{cb} . There have been many attempts to obtain the IWF in several models and different non-perturbative methods [5–8]. As the kinematic dependence of the IWF is unknown,

there exist different parameterizations of the IWF and different non-perturbative methods to calculate the value at zero recoil as well as the slope. In fact, in the heavy-quark symmetry the form factor can only depend on $\omega = v \cdot v'$, which connects the rest frames of the initial and final state mesons. Because of current conservation, this form factor is normalized to unity at zero recoil. The hadronic form factors of B to D meson transitions are among the important applications of the heavy-quark symmetry. In this limit, all form factors of B to D meson transitions can be analyzed via the IWF $\xi(\omega)$ of the velocity transfer ω [9]. Until now, valuable papers have been published and various aspects of formalism have been discussed. Bouzas and Gupta discussed the constraints on the IWF using sum rules for the B meson decays [10]. Charm and bottom baryons and mesons have been studied within the framework of the Bethe–Salpeter equation by Ivanov et al. They also reported the decay rates of charm and bottom baryons and mesons [11]. Kiselev determined the slope of the IWF and the $|V_{cb}|$ matrix element for semileptonic $B \rightarrow D\ell\nu$ decay [12]. The theory and phenomenology of weak decays of B mesons were reviewed by Neubert [13]. Leptonic decays of heavy pseudoscalar mesons and semileptonic decays of mesons were studied in Refs. [14, 15]. Ebert et al. studied the exclusive semileptonic decays of B mesons to orbitally excited D mesons in the framework of the relativistic quark model [16]. A lattice study of semileptonic B decays was presented by Bowler et al. (UKQCD collaboration) [17]. Measurements of the semileptonic Decays $B \rightarrow D\ell\nu$ were studied by Ref. [18] in 2008. Bernlochner et al. explored the rates of semileptonic B decays [19]. Atoui investigated the results of lattice QCD study of the exclusive semileptonic $B_s \rightarrow D_s\ell\nu$ decay form factors in the region near zero recoil [20]. The hadronic form factors of B semileptonic decays at both zero and nonzero recoil were computed by Qiu et al. [21].

The main aim of this manuscript is the study of the IWF for the B to D transition. In the next section, we will obtain the

^a e-mail: h.hasanabadi@shahroodut.ac.ir

mesonic wave function using the perturbation method. We then investigate the IWF for semileptonic B to D decay and present the slope, curvature, decay width, branching ratio, and $|V_{cb}|$ element of the CKM matrix in Sect. 3. Section 4 includes the numerical results and comparison with other models. The relevant conclusions are given in Sect. 5.

2 Mesonic wave function

As the IWF measures the overlap of the wave function of two hadrons, we have to first compute the wave function of the mesonic system. Our starting point is the three-dimensional radial Schrödinger equation possessing the form

$$-\frac{\hbar^2}{2\mu}\nabla^2\psi_{n,\ell}(r) + V(r)\psi_{n,\ell}(r) = E_{n,\ell}\psi_{n,\ell}(r) \tag{1}$$

where μ is the reduced meson mass and $E_{n,\ell}$ denotes the energy of the system. We choose the potential as

$$V(r) = -\frac{V_0}{e^{\alpha r} - 1} + br, \tag{2}$$

which is a combination of a linear confinement term and the Hulthén potential. The combination of confining and non-confining terms has successfully accounted for the phenomenological data. In fact, the linear term is the large distance confinement that arises from the color field flux tube between the quarks. The Hulthén potential is one of the important short-range potentials, which at short distances possesses asymptotic freedom, behaves like the Coulomb potential for small values of r , and decreases exponentially at large values. This behavior is in particular of interest in particle physics. Moreover, the potential has been used in other areas such as nuclear, atomic, solid-state, and chemical physics. As an example, it has been shown that the potential in the form $V_H = -\frac{V_0 e^{-\delta r}}{1 - e^{-\delta r}}$, where V_0 and δ , respectively, represent the strength and screening range of the potential, can acceptably account for description of interactions between the nucleon and heavy nuclei [22,23]. In our calculations, we consider the linear term as the parent;

$$H_0 = -\frac{\hbar^2}{2\mu}\nabla^2 + br, \tag{3}$$

and the Hulthén interaction therefore plays the role of the perturbation and the perturbed Hamiltonian is

$$H' = -\frac{V_0}{e^{\alpha r} - 1}. \tag{4}$$

As already mentioned, our parent Hamiltonian is ($\hbar = 1$)

$$\frac{d^2 u_{n,\ell}}{dr^2} - \frac{\ell(\ell+1)}{r^2} u_{n,\ell}(r) - 2\mu br u_{n,\ell}(r) = -2\mu E_{n,\ell} u_{n,\ell}(r). \tag{5}$$

Now let us limit the study to the ground state with $n = 1, \ell = 0$. The corresponding equation is [24]

$$\frac{d^2 u_{1,0}}{d\kappa^2} - \kappa u_{1,0} = 0, \tag{6}$$

which possesses the wave function

$$u_{1,0}(r) = N Ai[\kappa] \tag{7}$$

where κ is defined as

$$\kappa = (2\mu b)^{\frac{1}{3}} r - \left(\frac{2\mu}{b^2}\right)^{\frac{1}{3}} E_{1,0} \tag{8}$$

and Ai denotes the Airy function. The corresponding energy of the system is

$$E_{1,0} = -\left(\frac{b^2}{2\mu}\right)^{\frac{1}{3}} \kappa_0, \tag{9}$$

with κ_0 being the zero of the Airy function, which is -2.3194 in the case of the ground state ($1s$) [24]. Now, we calculate the perturbed wave function by using the first-order perturbation

$$H_0 \psi'_{1,0}(r) + H' u_{1,0}(r) = E_{1,0} \psi'_{1,0}(r) + w' u_{1,0}(r) \tag{10}$$

where

$$\psi'_{1,0}(r) = N' G(r) u_{1,0}(r) \tag{11}$$

and w' is the perturbed energy. Replacing Eqs. (3), (4), (11) into Eq. (10), we can write

$$\left[\frac{d^2}{dr^2} + \frac{2}{r} \frac{d}{dr} - 2\mu br + 2\mu E_{1,0} \right] G(r) = \left[-2\mu w' - \frac{2\mu V_0}{e^{\alpha r} - 1} \right] u_{1,0}(r). \tag{12}$$

We now propose

$$G(z) = \sum_{q=0}^{\infty} A_q z^q, \tag{13}$$

introduce the transformation $z = e^{-\alpha r}$, and use the approximation

$$\frac{1}{r^2} \approx \frac{\alpha^2}{(e^{\alpha r} - 1)^2} \tag{14}$$

to bring Eq. (12) into the form

$$\begin{aligned} & \sum_{q=0}^{\infty} q(q-1)A_q z^{q-2} - 2 \sum_{q=0}^{\infty} q(q-1)A_q z^{q-1} \\ & + \sum_{q=0}^{\infty} q(q-1)A_q z^q + \sum_{q=0}^{\infty} qA_q z^{q-2} - 2 \sum_{q=0}^{\infty} qA_q z^{q-1} \\ & + \sum_{q=0}^{\infty} qA_q z^q - 2(2\mu b)^{\frac{1}{3}} k_1 \sum_{q=0}^{\infty} qA_q z^{q-1} \\ & + 2(2\mu b)^{\frac{1}{3}} k_1 \sum_{q=0}^{\infty} qA_q z^q + (2\mu b)^{\frac{2}{3}} k_2 \sum_{q=0}^{\infty} A_q z^q \\ & - 2 \sum_{q=0}^{\infty} qA_q z^{q-1} + 2 \sum_{q=0}^{\infty} qA_q z^q + 2(2\mu b)^{\frac{1}{3}} k_1 \sum_{q=0}^{\infty} A_q z^q \\ & - \frac{2\mu b}{\alpha^3} \sum_{q=0}^{\infty} A_q z^{q-3} + \frac{6\mu b}{\alpha^3} \sum_{q=0}^{\infty} A_q z^{q-2} - \frac{6\mu b}{\alpha^3} \sum_{q=0}^{\infty} A_q z^{q-1} \\ & + \frac{2\mu b}{\alpha^3} \sum_{q=0}^{\infty} A_q z^q + \frac{2\mu E_{1,0}}{\alpha^2} \sum_{q=0}^{\infty} A_q z^{q-2} \\ & - \frac{4\mu E_{1,0}}{\alpha^2} \sum_{q=0}^{\infty} A_q z^{q-1} + \frac{2\mu E_{1,0}}{\alpha^2} \sum_{q=0}^{\infty} A_q z^q = -\frac{2\mu w'}{\alpha^2} z^{-2} \\ & + \frac{4\mu w'}{\alpha^2} z^{-1} - \frac{2\mu w'}{\alpha^2} - \frac{2\mu V_0}{\alpha^2} z^{-1} + \frac{2\mu V_0}{\alpha^2} \end{aligned} \tag{15}$$

with k_1, k_2, k considered to be [25]

$$\begin{aligned} k_1 &= 1 + \frac{k}{r}, \\ k_2 &= \frac{k^2}{r^2}, \\ k &= \frac{a_1 - b_1 \kappa_0}{b_1 (2\mu b)^{\frac{1}{3}}}, \end{aligned} \tag{16}$$

where $a_1 = 0.3550281, b_1 = 0.2588194$ are constants in Airy’s infinite polynomial [25]. Considering the z^{-3} coefficients of Eq. (15) we arrive at

$$A_0 = 0. \tag{17}$$

Equating the corresponding powers of z^{-2}, z^{-1}, z^0 on both sides of Eq. (15), we get A_1, A_2, A_3 , respectively:

$$A_1 = \frac{\alpha w'}{b}, \tag{18a}$$

$$A_2 = \frac{w'\alpha}{b} + \frac{\alpha^4 w'}{2\mu b^2} + \frac{V_0 \alpha}{b} + \frac{E_{1,0} \alpha^2 w'}{b^2}, \tag{18b}$$

$$\begin{aligned} & -4A_1 - 2(2\mu b)^{\frac{1}{3}} k_1 A_1 - \frac{6\mu b}{\alpha^3} A_1 - \frac{4\mu E_{1,0}}{\alpha^2} A_1 + 4A_2 \\ & + \frac{6\mu b}{\alpha^3} A_2 + \frac{2\mu E_{1,0}}{\alpha^2} A_2 - \frac{2\mu b}{\alpha^3} A_3 = -\frac{2\mu w'}{\alpha^2} + \frac{2\mu V_0}{\alpha^2}. \end{aligned} \tag{18c}$$

As a result, we have

$$\psi'_{1,0}(r) = N' (A_0 + A_1 z + A_2 z^2 + A_3 z^3) u_{1,0}(r). \tag{19}$$

Thus the total wave function has the form

$$\psi_{1,0}^{\text{tot}}(r) = N^{\text{tot}} [u_{1,0}(r) + \psi'_{1,0}(r)] \tag{20}$$

where N^{tot} is the normalization constant of the total wave function. We now go through the semileptonic decay $\bar{B} \rightarrow D\ell\bar{\nu}$ within the IWF approach.

3 Isgur–Wise function, decay width, and branching ratio of $\bar{B} \rightarrow D\ell\bar{\nu}$ decay

The IWF is often written as

$$\xi(\omega) = 1 - \rho^2(\omega - 1) + C(\omega - 1)^2 + \dots, \tag{21}$$

which is well supported by the experimental data [26,27] where the velocity transfer $\omega = v_B \cdot v_D$ is the dot product of the four-velocities of the B and D mesons. On the other hand, the kinematic accessible region in the semileptonic decays is limited to $\omega = 1$ to 1.43. Thus, most studies consider the IWF in the vicinity of the zero-recoil point ($\omega = 1$). The IWF for mesons can be written in terms of the integral [28]

$$\xi(\omega) = \int_0^{\infty} 4\pi r^2 |\psi_{1,0}^{\text{tot}}(r)|^2 \cos(pr) dr, \tag{22}$$

which depends on the momentum transfer ($p^2 = 2\mu^2(\omega - 1)$). Because of the implication of the current conservation of the form factor, the IWF is normalized to unity at $p^2 = 0$, which corresponds to $\omega = 1$ demonstrating the zero-recoil limit [13]. Extending $\cos(pr)$ and comparing Eqs. (21) and (22), we find the so-called slope and curvature parameters as

$$\rho^2 = 4\pi\mu^2 \int_0^{\infty} r^4 |\psi_{1,0}^{\text{tot}}(r)|^2 dr, \tag{23a}$$

$$C = \frac{2}{3}\pi\mu^4 \int_0^{\infty} r^6 |\psi_{1,0}^{\text{tot}}(r)|^2 dr, \tag{23b}$$

where ω is referred to as the mesonic zero-recoil point. In Fig. 1, the behavior of the IWF for some B and D mesons is plotted. The differential semileptonic decay width of $\bar{B} \rightarrow D\ell\bar{\nu}$ in the heavy-quark limit has the form [13]

$$\begin{aligned} & \frac{d\Gamma(\bar{B} \rightarrow D\ell\bar{\nu})}{d\omega} \\ & = \frac{G_F^2}{48\pi^3} |V_{cb}|^2 (m_B + m_D)^2 m_D^3 (\omega^2 - 1)^{\frac{3}{2}} \xi^2(\omega) \end{aligned} \tag{24}$$

where V_{cb} is the element of CKM matrix. Equation (24) indicates the dependence of the differential semileptonic decay

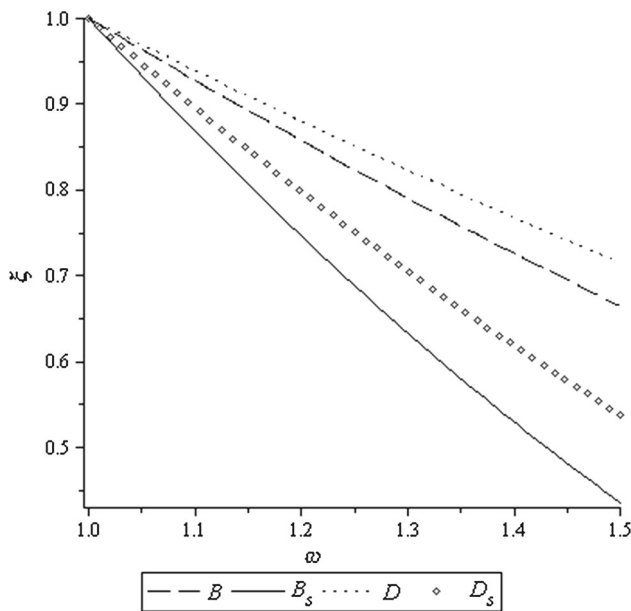


Fig. 1 Variation of IWF for some B, D mesons

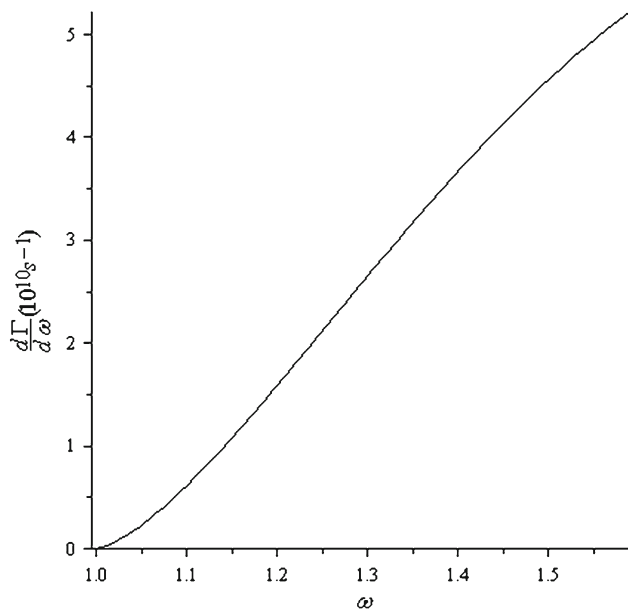


Fig. 2 Differential decay width vs. ω for $\bar{B} \rightarrow D\ell\bar{\nu}$

width on the ω parameter and the product of four-velocities of two mesons in $B \rightarrow D$ transition. We have plotted $\frac{d\Gamma}{d\omega}$ versus ω for $\bar{B} \rightarrow D\ell\bar{\nu}$ semileptonic decay in Fig. 2. By integrating of differential decay width over the interval $1 \leq \omega \leq \frac{m_B^2 + m_D^2}{2m_B m_D}$, we calculate the decay width of $\bar{B} \rightarrow D\ell\bar{\nu}$ decay. In addition, we obtain the decay width of $\bar{B}_s \rightarrow D_s\ell\bar{\nu}$ using the same approach. Figure 3 presents the variation of $\frac{d\Gamma}{d\omega}$ vs. ω for $\bar{B}_s \rightarrow D_s\ell\bar{\nu}$ semileptonic decay. Table 1 shows our calculated slope and curvature for D and B heavy-light mesons. We have shown our results for decay width, branch-

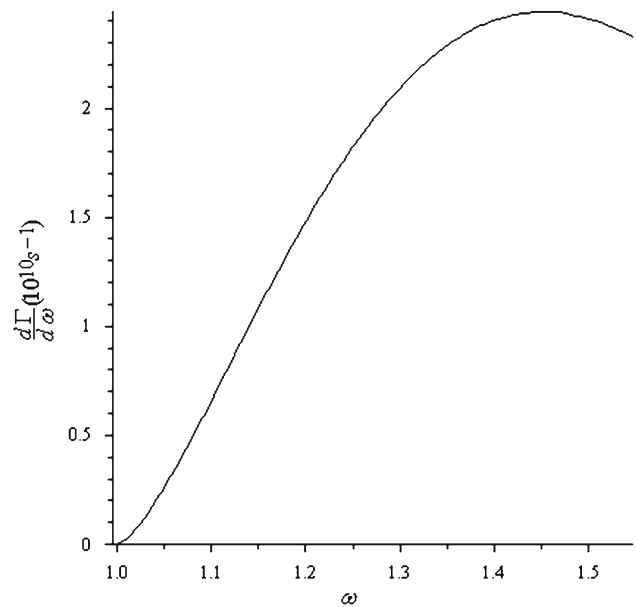


Fig. 3 Differential decay width vs. ω for $\bar{B}_s \rightarrow D_s\ell\bar{\nu}$

Table 1 Slope, curvature of IWF for B, D, B_s, D_s mesons ($V_0 = -1.61 \text{ GeV}$, $\alpha = 0.1 \text{ GeV}$, $b = 0.76 \text{ GeV}^2$ for B, D and $V_0 = -1.61 \text{ GeV}$, $\alpha = 0.1 \text{ GeV}$, $b = 0.6 \text{ GeV}^2$ for B_s, D_s)

Meson	ρ^2 (ours)	ρ^2 (others)	Uncertainty (%)	C (ours)
B ($\mu_B = 0.314$)	0.74	0.70 [25]	5.7	0.13
D ($\mu_D = 0.276$)	0.62	0.68 [25]	8.8	0.09
B_s ($\mu_{B_s} = 0.440$)	1.36	1.46 [32]	6.8	0.46
D_s ($\mu_{D_s} = 0.368$)	1.06	1.19 [20]	10.9	0.28

ing ratio, and the element of the CKM matrix for $\bar{B} \rightarrow D\ell\bar{\nu}$ decay in Table 2. We have tabulated our mentioned results for $\bar{B}_s \rightarrow D_s\ell\bar{\nu}$ decay in Table 3. In the first column of Table 1 we have shown B and D mesons with their reduced mass which are our input assumptions. In the second and fifth columns we have shown our results for slope (ρ^2) and curvature (C), respectively, by using Eqs. (23) in our calculations. In the third column, we have shown the reported values of other models for ρ^2 . The fourth column indicates uncertainties for our obtained values of the slope parameter. Integrating Eq. (24) we have presented our results for $\bar{B} \rightarrow D\ell\bar{\nu}$ and $\bar{B}_s \rightarrow D_s\ell\bar{\nu}$ decays in Tables 2 and 3, respectively. We have included our integrated decay width using the input parameters mentioned in Sect. 4. The tables also includes the branching ratio for $\bar{B} \rightarrow D\ell\bar{\nu}$ and $\bar{B}_s \rightarrow D_s\ell\bar{\nu}$. We have presented the extracted $|V_{cb}|$ in the fourth row of the second column of Tables 2 and 3. We have compared our results for decay width, branching ratio, and $|V_{cb}|$ quantities with other models in the third column of Table 2. We have obtained the uncertainty of the mentioned quantities in the fourth column of Table 2 for $\bar{B} \rightarrow D\ell\bar{\nu}$ decay and the third column of Table 3 for $\bar{B}_s \rightarrow D_s\ell\bar{\nu}$ decay, respectively. Dis-

Table 2 Decay width, branching ratios, and $|V_{cb}|$ for $\bar{B} \rightarrow D\ell\bar{\nu}$

Quantity	Our model	Other models	Uncertainty (%)
Γ (in $10^{10} s^{-1}$)	1.51	1.413 [12] 1.43 \pm 0.08 [18]	6.8 5.5
Br (in %)	2.48	2.23 \pm 0.12 [29] 2.31 \pm 0.09 [19] 2.34 \pm 0.03 \pm 0.13 [18]	11.2 7.3 5.9
$ V_{cb} $	$0.037 \leq V_{cb} \leq 0.039$	0.042 \pm 0.001 [29]	7.1–11.9

Table 3 Decay width, branching ratios, and $|V_{cb}|$ for $\bar{B}_s \rightarrow D_s\ell\bar{\nu}$

Quantity	Our model	Uncertainty (%)
Γ (in $10^{10} s^{-1}$)	0.89	4.3
Br (in %)	1.35	2.7
$ V_{cb} $	0.038	7.3

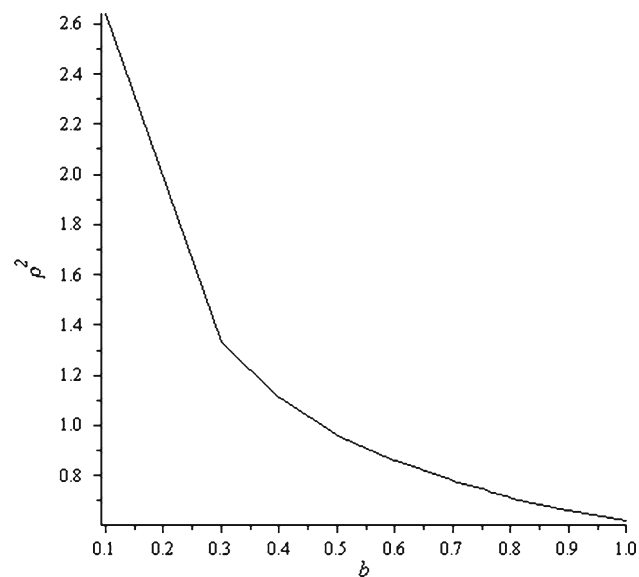


Fig. 4 ρ^2 vs. $b(\text{GeV}^2)$ for $V_0 = -1.61 \text{ GeV}$, $\alpha = 0.1 \text{ GeV}$

cussions on the reported results are in the next section. As we know, the branching ratio of heavy-light meson decays obeys

$$Br = \Gamma\tau. \tag{25}$$

Therefore, using the obtained decay width and the heavy-light meson lifetime as $\tau_B = 1.64\text{ps}$ [29] and $\tau_{B_s} = 1.51\text{ps}$ [29], we are able to calculate the corresponding branching ratios reported in the third row of Tables 2 and 3.

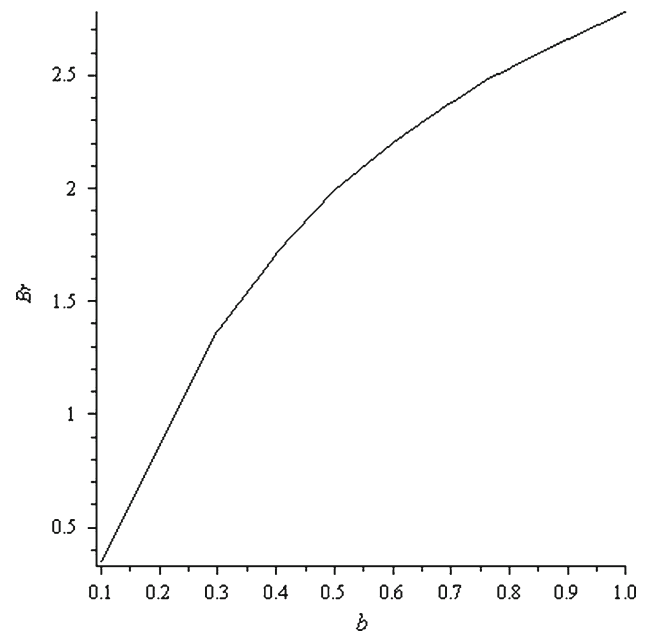


Fig. 5 $Br(\bar{B} \rightarrow D\ell\bar{\nu})$ vs. $b(\text{GeV}^2)$ for $V_0 = -1.61 \text{ GeV}$, $\alpha = 0.1 \text{ GeV}$

4 Results and discussion

The masses of bottom and charmed B and D mesons are taken as $m_{\bar{B}} = 5.279 \text{ GeV}$, $m_D = 1.869 \text{ GeV}$, $m_{\bar{B}_s} = 5.366 \text{ GeV}$ and $m_{D_s} = 1.968 \text{ GeV}$ in the calculations [29]. We have chosen the potential parameters as $V_0 = -1.61 \text{ GeV}$, $\alpha = 0.1 \text{ GeV}$, $b = 0.76 \text{ GeV}^2$ for $\bar{B} \rightarrow D\ell\bar{\nu}$ and $V_0 = -1.61 \text{ GeV}$, $\alpha = 0.1 \text{ GeV}$, $b = 0.6 \text{ GeV}^2$ for $\bar{B}_s \rightarrow D_s\ell\bar{\nu}$. We have plotted the variation of the slope parameter and $Br(\bar{B} \rightarrow D\ell\bar{\nu})$ vs. $b(\text{GeV}^2)$ when $V_0 = -1.61 \text{ GeV}$, $\alpha = 0.1 \text{ GeV}$ are kept constant in Figs. 4 and 5, respectively. Furthermore, we have plotted the slope parameter and $Br(\bar{B} \rightarrow D\ell\bar{\nu})$ vs. $\alpha(\text{GeV})$ when $V_0 = -1.61 \text{ GeV}$, $b = 0.76 \text{ GeV}^2$ are kept constant in Figs. 6 and 7, respectively. The results of Table 1 are compatible with the available experimental and theoretical values. Faller et al. reported $\rho^2 = 0.81 \pm 0.22$ [9]. Adopting the used form of the IWF in the previous section, we get $\rho^2 = 0.74$ for the B meson, which is in the vicinity of the result of QCD sum rule, which predicted $\rho^2 = 0.65$ [7]. Sadzikowski and Zalewski reported $\rho_{B_s}^2 = 1.62$ for the slope of B_s meson [30]. Our result $\rho^2 = 1.36$ is in agreement with their work. Ebert et al. [16] reported the decay width and the branching ratio of B to D decay as: $\Gamma = 2.7 | \frac{V_{cb}}{0.04} |^2 10^{-15} \text{ GeV}$ and (0.63 in %), respectively. Considering $V_{cb} = 0.04$, Γ will be 0.41 (in $10^{10} s^{-1}$) [16] and our calculations are comparable with them. Moreover, our obtained quantity for $Br(\bar{B} \rightarrow D\ell\bar{\nu}) = 2.48$ is in good agreement with reports of the ARGUS, CLEO, and UKQCD collaboration, which are $Br(\bar{B} \rightarrow D\ell\bar{\nu}) = 2.1 \pm 0.7 \pm 0.6$ [31], $Br(\bar{B} \rightarrow D\ell\bar{\nu}) = 1.8 \pm 0.6 \pm 0.3$ [31] and $Br(\bar{B} \rightarrow D\ell\bar{\nu}) = 1.5_{-4}^{+4} \pm 0.3$,

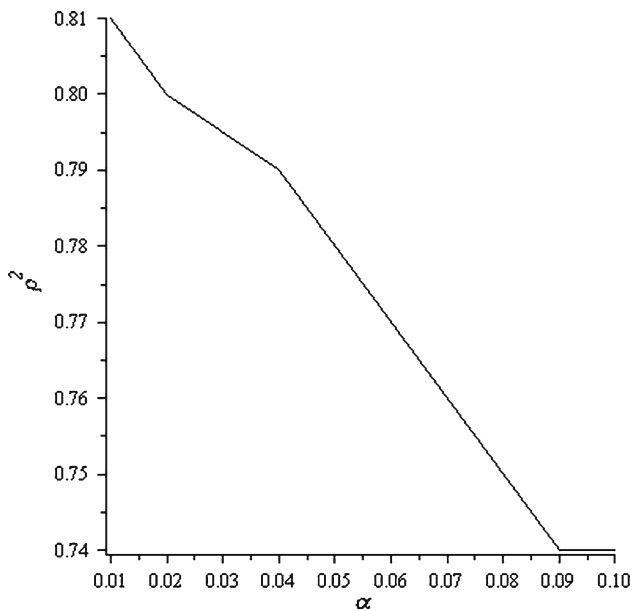


Fig. 6 ρ^2 vs. $\alpha(\text{GeV})$ for $V_0 = -1.61 \text{ GeV}$, $b = 0.76 \text{ GeV}^2$

respectively [17]. The UKQCD collaboration [17] reported $Br(\bar{B}_s \rightarrow D_s \ell \bar{\nu}) = 1.3_{-2}^{+2} \pm 0.3$. Considering $\tau_{B_s} = 1.51 \text{ ps}$ [29], the value of the decay width for the UKQCD collaboration is $\Gamma = 0.86 \times 10^{10} \text{ s}^{-1}$. Our values for this decay are in agreement with them. Moreover, our results for $\bar{B}_s \rightarrow D_s \ell \bar{\nu}$ decay are in good agreement with the result of Faustov and Galkin ($Br(\bar{B}_s \rightarrow D_s \ell \bar{\nu}) = 2.1 \pm 0.2$) [32], ($Br(\bar{B}_s \rightarrow D_s \ell \bar{\nu}) = 1.4$) of the work of Chen et al. [33] and ($Br(\bar{B}_s \rightarrow D_s \ell \bar{\nu}) = 1.0_{-0.3}^{+0.4}$) the reported value of Li et al. [34]. We have obtained $\Gamma(B \rightarrow D \ell \bar{\nu}) = 945.76 \times 10^{10} \text{ s}^{-1} |V_{cb}|^2$ and $Br(B \rightarrow D \ell \bar{\nu}) = 1551.05 |V_{cb}|^2$ for semileptonic B decay. For semileptonic B_s decay we can calculate $\Gamma(B_s \rightarrow D_s \ell \bar{\nu}) = 561.59 |V_{cb}|^2 \times 10^{10} \text{ s}^{-1}$ and $Br(B_s \rightarrow D_s \ell \bar{\nu}) = 848.00 |V_{cb}|^2$. To extract $|V_{cb}|$, we have used the reported values of integrated decay width of B to D semileptonic decays from Refs. [18,20] and substituted them in the integrated decay width. We also applied the IWF (Eq. (21)) as well as Eqs. (23) of Sect. 3. As we know, the differential decay rate for the process $B \rightarrow D \ell \nu$ is given by [21]

$$\begin{aligned} \frac{d\Gamma}{d\omega}(B \rightarrow D \ell \nu) &= |\bar{\eta}_{EW}|^2 \frac{G_F^2}{48\pi^3} |V_{cb}|^2 (m_B + m_D)^2 m_D^3 (\omega^2 - 1)^{\frac{3}{2}} \xi^2(\omega) \end{aligned} \tag{26}$$

where the factor $|\bar{\eta}_{EW}|^2$ accounts for electroweak corrections. When fitting to the experimental data, it is necessary to bear in mind that the electroweak effects are present in the experimental values but not included in the lattice calculation. Therefore, the factor $\bar{\eta}_{EW} = 1.011$ is included in the calculations and the ratio of experimental to theoretical val-

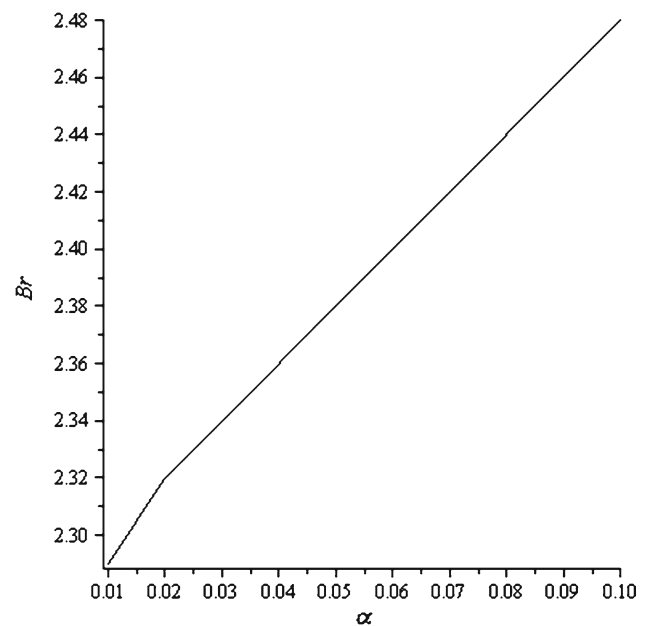


Fig. 7 $Br(\bar{B} \rightarrow D \ell \bar{\nu})$ vs. $\alpha(\text{GeV})$ for $V_0 = -1.61 \text{ GeV}$, $b = 0.76 \text{ GeV}^2$

ues must be divided by $\bar{\eta}_{EW}$ to get $|V_{cb}|$ [21]. We have taken into account the electroweak effects to extract $|V_{cb}|$ using $\bar{\eta}_{EW} = 1.011$ [21] in Eq. (26). We use the parameterization of Ref. [20], thus

$$\frac{\xi(\omega)}{\xi(1)} = 1 - 8\rho^2 z + (51\rho^2 - 10)z^2 - (252\rho^2 - 84)z^3. \tag{27}$$

Our input assumptions are $\xi(1) = 1.052$, $z = \frac{\sqrt{\omega+1}-\sqrt{2}}{\sqrt{\omega+1}+\sqrt{2}}$, $\rho^2 = 1.2$, $m_{\bar{B}_s} = 5.366 \text{ GeV}$, $m_{D_s} = 1.968 \text{ GeV}$, $|V_{cb}| = 0.04$. By replacing $\xi(\omega)$ from Eq. (27) in the equation

$$\begin{aligned} \frac{d\Gamma(\bar{B}_s \rightarrow D_s \ell \bar{\nu})}{d\omega} &= \frac{G_F^2}{48\pi^3} |V_{cb}|^2 (m_{B_s} + m_{D_s})^2 m_{D_s}^3 (\omega^2 - 1)^{\frac{3}{2}} \xi^2(\omega) \end{aligned}$$

and adopting the above-mentioned input assumptions after integrating over the range $1 \leq \omega \leq \frac{m_{\bar{B}_s}^2 + m_{D_s}^2}{2m_{B_s} m_{D_s}}$, we obtain $\Gamma = 1.43 \times 10^{10} \text{ s}^{-1}$ [20]. In the case of this value of the decay width for $\bar{B}_s \rightarrow D_s \ell \bar{\nu}$ we obtain $|V_{cb}| = 0.050$. Employing the experimental decay width ($\Gamma = (1.43 \pm 0.08) \times 10^{10} \text{ s}^{-1}$) for $\bar{B} \rightarrow D \ell \bar{\nu}$ [18] and using our presented model, we report CKM matrix ($|V_{cb}|$) as $0.037 \leq |V_{cb}| \leq 0.039$ with uncertainty of 7.1–11.9%. Our obtained uncertainties are between 4.6 and 13.8 in Table 1. The decay width, branching ratio, and V_{cb} have 5.5, 5.9, 7.1 (in percent) uncertainties for $\bar{B} \rightarrow D \ell \bar{\nu}$, respectively, in our model as can be seen in Table 2. For the mentioned quantities in the case of $\bar{B}_s \rightarrow D_s \ell \bar{\nu}$ decay we have obtained 4.3, 2.7, 7.3 uncertainties as shown in Table 3. The advantage of our model is its simplicity.

5 Conclusions

We considered a mesonic system influenced by linear and Hulthén interactions. Next, using the perturbation technique, and the Isgur–Wise formalism, we obtained the corresponding decay width and branching ratios for some B to D decays. The results are in good agreement with experimental values and other models. Our model is also simple, with no intricacies of a mathematical nature.

Acknowledgments The authors would like to thank the referee for giving valuable suggestions and criticisms improving the paper.

Open Access This article is distributed under the terms of the Creative Commons Attribution License which permits any use, distribution, and reproduction in any medium, provided the original author(s) and the source are credited.

Funded by SCOAP³ / License Version CC BY 4.0.

References

1. N. Isgur, M.B. Wise, Phys. Lett. B **232**, 113 (1989)
2. N. Isgur, M.B. Wise, Phys. Lett. B **237**, 527 (1990)
3. N.B. Demchuk, JHEP **08**, 008 (1998)
4. M.G. Olsson, S. Veseli, Phys. Rev. D **51**, 2224–2229 (1995)
5. B. Holdom, M. Sutherland, J. Mureika, Phys. Rev. D **49**, 2359 (1994)
6. M.A. Ivanov, V.E. Lyubovitskij, J.G. Körner, P. Kroll, Phys. Rev. D **56**, 348 (1997)
7. Y.B. Dai, C.S. Huang, M.Q. Huang, C. Liu, Phys. Lett. B **387**, 379 (1996)
8. E. Jenkins, A. Manohar, M.B. Wise, Nucl. Phys. B **396**, 38 (1996)
9. S. Faller, A. Khodjamirian, Ch. Klein, Th Mannel, Eur. Phys. J. C **60**, 603–615 (2009)
10. A.O. Bouzas, V. Gupta, J. Phys. G **24**, 2023 (1998)
11. M.A. Ivanov, J.G. Körner, V.E. Lyubovitskij, A.G. Rusetsky, Phys. Rev. D **59**, 074016 (1999)
12. V.V. Kiselev, Mod. Phys. Lett. A **10**, 1049 (1995)
13. M. Neubert, Int. J. Mod. Phys. A **11**, 4173 (1996)
14. S.S. Gershtein, M.Yu. Khlopov, Pis'ma v ZhETF **23**, 374–377 (English translation: JETPLett. 23(1976) 338–340) (1976)
15. M.Yu. Khlopov, Yadernaya Fizika **28**, 1134–1137 (English translation: Sov. J. Nucl. Phys. 28 (1978) 583–584) (1978)
16. D. Ebert, R.N. Faustov, V.O. Galkin, Phys. Rev. D **61**, 014016 (2000)
17. K.C. Bowler et al., UKQCD collaboration. Phys. Rev. D **52**, 5067 (1995)
18. B. Aubert et al., The BABAR collaboration. Phys. Rev. D **79**, 012002 (2009)
19. F.U. Bernlochner, Z. Ligeti, S. Turczyk, Phys. Rev. D **85**, 094033 (2012)
20. M. Atoui, D. Becirevic, V. Morenas, F. Sanfilippo, arXiv:1310.5238
21. S. W. Qiu, C. DeTar, A. X. El-Khadra, A. S. Kronfeld, J. Laiho, R. S. Van de Water, arXiv:1312.0155
22. N. Saad, Phys. Scr. **76**, 623 (2007)
23. L. Hulthen, Ark. Mat. Astron. Fys. **28**, A5 (1942)
24. I.J.R. Aitchison, J.J. Dudek, Eur. J. Phys. **23**, 605 (2002)
25. S. Roy, N.S. Bordoloi, D.K. Choudhury, Can. J. Phys. **91**, 34 (2013)
26. T. Coleman, M.G. Olsson, S. Veseli, Phys. Rev. D **63**, 032006 (2001)
27. B. Aubert et al., The BABAR collaboration. Phys. Rev. Lett. **104**, 011802 (2010)
28. H. Hassanabadi, S. Rahmani, S. Zarrinkamar, Phys. Rev. D **89**, 114027 (2014)
29. J. Beringer et al. PDG, Phys. Rev. D **86**, 010001 (2012)
30. M. Sadzikowski, K. Zalewski, Z. Phys. C **59**, 677 (1993)
31. “Semi-leptonic B Decays”, S. Stone, “B Decays”, ed. by S. Stone, 2nd edn. World Scientific, Singapore (1994)
32. R.N. Faustov, V.O. Galkin, Phys. Rev. D **87**, 034033 (2013)
33. X.J. Chen, H.F. Fu, C.S. Kim, G.L. Wang, J. Phys. G **39**, 045002 (2012)
34. R.-H. Li, C.-D. Lu, Y.-M. Wang, Phys. Rev. D **80**, 014005 (2009)